

## INFLUENCE OF SURFACE QUALITY ON FATIGUE BEHAVIOR OF NODULAR CAST IRON

*M. Kokavec<sup>1</sup>, R. Konečná<sup>1</sup>, G. Nicoletto<sup>2</sup>*

*<sup>1</sup>Department of Materials Engineering, University of Žilina, Slovakia*

*<sup>2</sup>Department of Industrial Engineering, University of Parma, Italy*

Received 14.10.2010

Accepted 28.03.2011

*Corresponding author: M. Kokavec, Telephone number: 041/513 2632, Department of Materials Engineering, Faculty of Mechanical Engineering, University of Žilina, Slovakia, E-mail: marian.kokavec@fstroj.uniza.sk*

### Abstract

The fatigue behavior of a component is strongly dependent on the material and its surface condition (surface roughness, residual stresses etc.). The paper presents and discusses the influence of the surface finish on the fatigue behavior of nodular cast iron. The fatigue properties were investigated on specimens with as-cast, shot-blast, fine-ground and rough-ground surface conditions under reversed bending loading. Selected fracture surfaces were investigated to determine fracture micro mechanisms associated to the different fatigue lives. The results show a large fatigue life scatter for all the investigated stress amplitudes which can be associated with the features of the surface finish at the origin of the formation of the main fatigue crack.

**Keywords:** iron alloys, fatigue test, bending test

### 1 Introduction

Nodular cast iron (NCI) is a construction material with a wide range of applications in engineering practice. For optimal application of NCI it is important to know its basic mechanical properties and the available methods to improve them [1]. Because the structure of nodular cast iron (NCI) contains graphite and casting defects, its fatigue strength is lower than that of steel, which has hardness almost equal to that of nodular cast iron (NCI). The fatigue properties of NCI are influenced by the matrix structure, the percentage of nodular graphite, and the presence of geometrical notches [2, 3, 4]. Slightly higher percentages of nodular graphite increase the fatigue strength as well as the endurance limit [5, 6]. The presence of a larger amount of pearlite in the matrix structure also increased the fatigue strength. The effect of matrix structure on the fatigue strength is less pronounced and the fatigue strength is significantly lower in the presence of notches [7, 8].

Since fatigue resistance is sensitive to surface conditions, any phenomenon that changes the surface characteristics of a material will greatly affect its fatigue performance [1]. Most structural engineering parts do not have highly polished surfaces and grinding or machining, even if done carefully, will cause degradation in fatigue strength. In general, fatigue life increases as the magnitude of surface roughness decreases or the surface hardness increases as in the case of surface treatments [9, 10].

A cost-effective cast part is obtained by reducing machining to a minimum, so the highest working stresses often develop at as-cast surfaces. Fatigue strength of NCI with as-cast surfaces is influenced by various factors such as : i) surface roughness or stress raisers, ii) changes in the

mechanical properties of the metal surface, and iii) changes in the residual stress condition near the surface. As these factors jointly influence fatigue damage development, the quantitative evaluation of the fatigue strength of NCI having as-cast surfaces is complex, resulting in different fatigue strength from that observed for smooth specimens [6, 8].

This paper presents a study of the fatigue behavior of pearlite/ferrite NCI specimens having different surface quality, namely as-cast, rough-ground, fine-ground and shot-blast. To highlight the dependence of the fatigue behavior on surface condition, specimens were cyclic tested under plane bending so that the maximum stress is reached at the surface of interest.

## 2 Material and experiments

The experimental material was made with a 2000 kg pig iron, 300 kg steel scrap, 1500 kg cast iron scrap. Melting was performed using an arched alkaline furnace. The experimental material was treated during heating with addition of 35 kg FeSi [11, 12]. Chemical composition of the pearlite-ferrite NCI is given in **Table 1**.

**Table 1** Chemical composition of pearlite-ferrite NCI, [%]

C	Si	Mn	S	P	Mg	Cr	Cu	Ni
3.68	2.62	0.51	0.005	0.05	0.034	0.2	0.02	0.01

The material was supplied in the form of plates with dimensions of 138x101x21 mm, from which the cutting operation produced specimens for the tensile and fatigue testing. The shape and dimensions of specimens for fatigue tests are shown in **Fig. 1**.

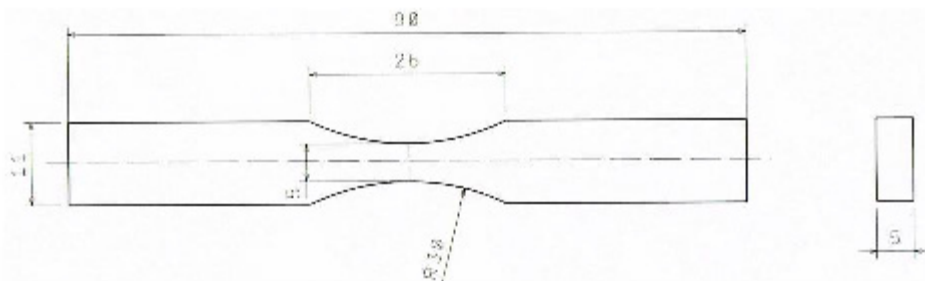


**Fig. 1** Shape and dimensions of specimen

The fatigue specimens were prepared by machining from cast plates. The load ratio of the fatigue test was selected as  $R = 0$ , so that one surface was subjected to a tensile stress range (the most critical in fatigue) and the opposite surface to a compressive stress range. The specimens marked as “As - cast” (**Fig. 2a**) had one test surface in the as-cast condition, the other ground. Specimens indicated as “Shot blast” (**Fig. 2b**) had the test surface shot blast after machining, specimens “Fine-ground” (**Fig. 2c**) had a smooth finish of the test surface achieved by removing casting surfaces by soft grinding and specimens “Rough-ground” (**Fig. 2d**) had a surface finish achieved by removing casting surfaces by rough grinding.

The structural analysis was performed on polished and etched specimens taken from casting plates. Structure details were analyzed in the light metallographic microscope according to the EN STN 42 0461 standard and by the methods of quantitative metallography [13].

The fatigue curves for specimens of NCI with different surface conditions were obtained on a cyclic plane bending testing machine operating at 25 Hz (i.e. load ratio  $R = 0$ ) in displacement-control [14]. The specimens were subjected to bending moment  $M = P \times L_0$  where  $P$  is the force monitored by a load cell and  $L_0$  the distance between the load cell and an internal support. Tests were interrupted at  $2 \cdot 10^6$  cycles if the specimen did not fail.

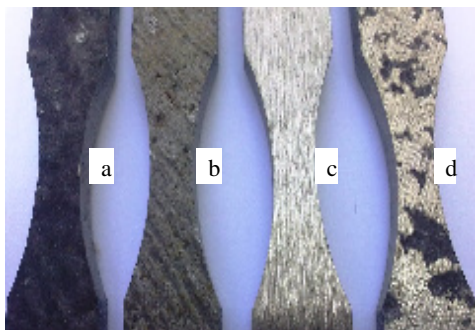


Fig. 2 Surface condition of specimens

### 3 Results and discussion

The structure of NCI was characterized by pearlite-ferrite matrix, **Fig. 3**, with higher content of pearlite in the matrix. The graphite nodules were observed in fully and partly not fully globular shape and there were located in ferritic part of matrix. Size was predominately ranging from 30 to 60  $\mu\text{m}$  (VI 6) and with a small number of nodules ranging in the size from 60 to 120  $\mu\text{m}$  (VI 5). Graphite nodule count  $N$  was in average 260  $\text{mm}^{-2}$ . The mechanical properties of studied NCI were  $R_m = 576 \text{ MPa}$  and  $A = 6 \%$ .

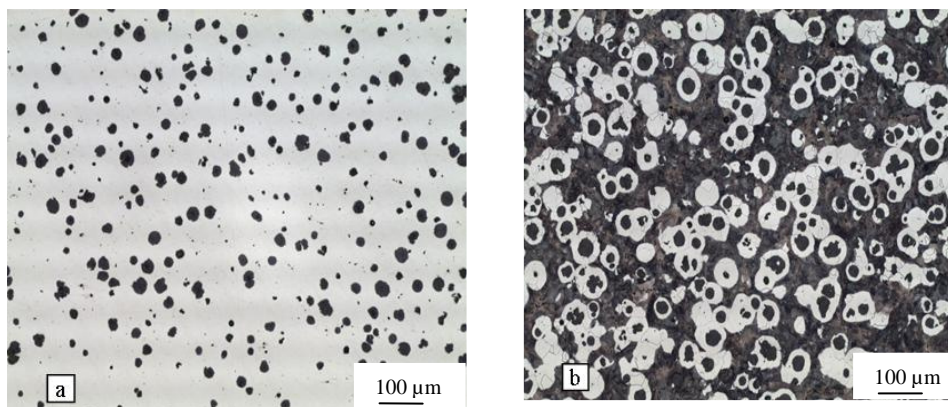
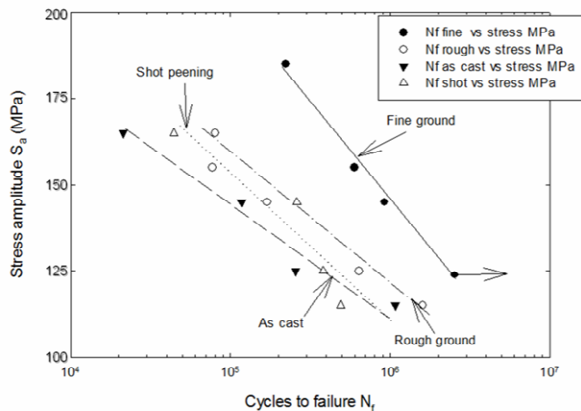


Fig.3 Microstructure of nodular cast iron, a) non etched, b) etched with 3% Nital

Fatigue test results corresponding to all the specimens at  $R = 0$  are presented in **Fig. 4**, where the number of cycles to failure is plotted vs. the stress amplitude  $\sigma_a$  (i.e.  $\sigma_{\text{max}}/2$ ). The results show a scatter in fatigue life for all the investigated stress amplitudes, which can be associated with the features of the surface finishing at the origin of the formation of the main fatigue crack. As expected, specimens with fine-ground surfaces achieve the highest fatigue endurance limit

compared to the other specimens with surfaces of higher roughness. Trends of S-N curves of specimens with rough-ground and shot-penned surfaces showed very similar behavior and had the highest scatter. The worst fatigue properties are determined in specimens with as-cast surfaces. The S-N curves confirm the effect of surface finishing on fatigue lives i.e. improvement as the surface becomes smoother [6].



**Fig. 4** Fatigue tests results (cyclic bending at  $R=0$ )

The fatigue fracture surfaces of selected specimens were analyzed in SEM to find initiation places of fatigue crack and to describe fracture mechanisms of the different structural components, ferrite and pearlite [2, 3, 15]. The initiation places were on the top of fracture surfaces, which were different in the dependence of stage production (**Fig. 5**). Transcrystalline cleavage of ferrite and pearlite was characteristic on the places near the surfaces [16].

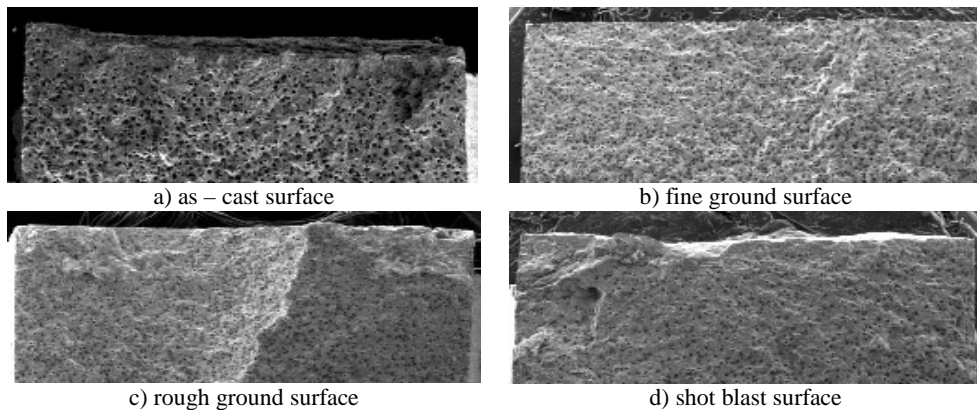


**Fig.5** The initiation areas on the surface top

Also longitudinal sectioning of the specimens allows an evaluation of surface roughness and surface features for the different qualities. As-cast specimens have a surface layer with casting sand and an initiation thickness near the surface is without nodules (**Fig. 5a**). The thickness of surface layer was not uniform. The fine ground specimens have nodules up to the surface (**Fig. 5b**). In the shot-blast specimen, **Fig. 5d**, only the as-cast surface layer was eliminated. The

rough-ground surface, **Fig. 5c**, is similar to the shot-blast surface, but occasionally can be seen graphite nodules on the surface.

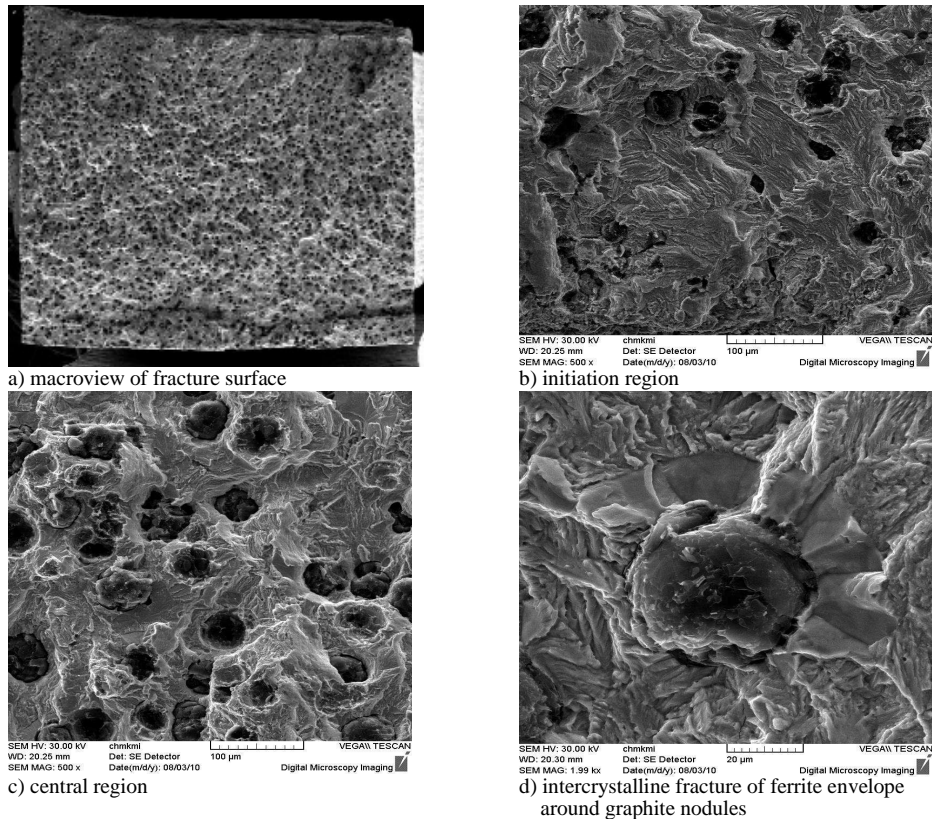
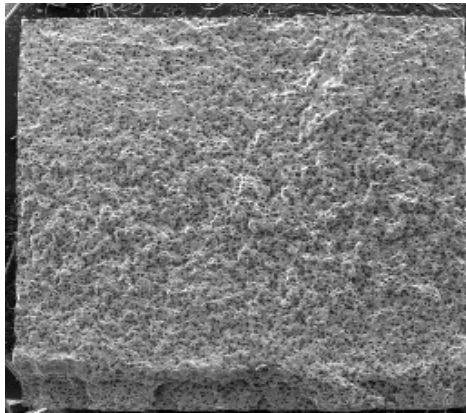


**Fig. 6** Fracture surface of As – cast specimens.,  $S = 290 \text{ MPa}$ ,  $N_f = 117\,475$ , SEM

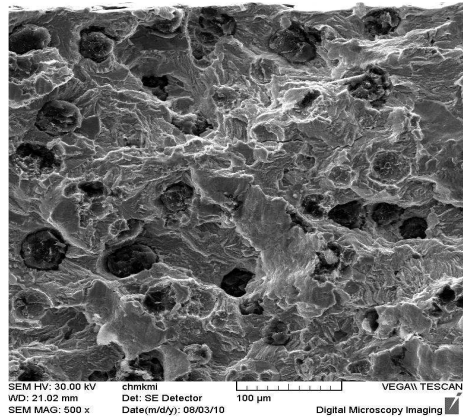
A macroview of the fracture surface of the as-cast specimen is shown in **Fig. 6a**. The initiation region near the surface is characterized by a typical transcrystalline cleavage of ferrite with smooth facets, **Fig. 6b**. Locally, envelopes of ferrite around graphite nodules, which failed by intercrystalline fracture, were observed. Transcrystalline ductile fracture of ferrite with dimples around graphite particles was found, **Fig. 6c**. In the region of final static fracture, the crack propagated by intercrystalline fracture of ferrite around graphite nodules while transcrystalline discontinuous cleavage was typical of pearlite, **Fig. 6d**.

For specimens with fine ground surfaces **Fig. 7a** and **7b**, fatigue cracks initially propagated by transcrystalline cleavage of ferrite and pearlite. Then, the fatigue crack growth mechanisms were similar to the as-cast specimens.

A macroview of the fracture surfaces of the rough ground and shot blast specimens are shown in **Fig. 8a, c**. In the initiation region of rough ground and shot blast specimens local intercrystalline fracture of ferrite were typical, transcrystalline continuous cleavage of pearlite with rivers on the facets was found in the specimens with the surface after rough ground and shot blast surface, **Fig. 8b, d**. The cracks in envelopes of ferrite around the graphite nodule propagated by intercrystalline fracture of ferritic grains and also regions with transcrystalline ductile fracture of ferrite with sharp edges were found, **Fig. 8d**.

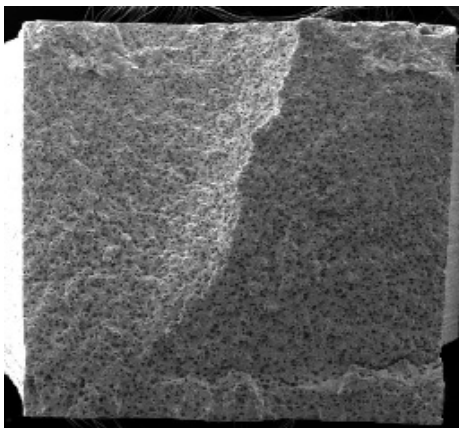


a) macroview of fracture surface

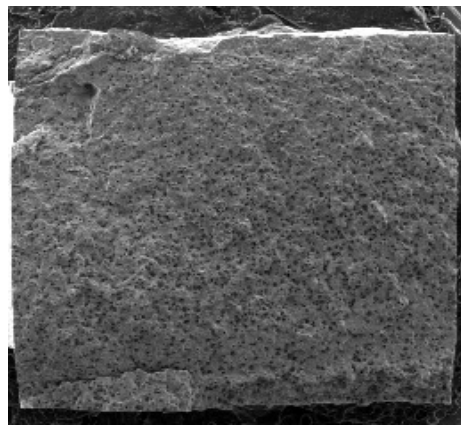


b) initiation region

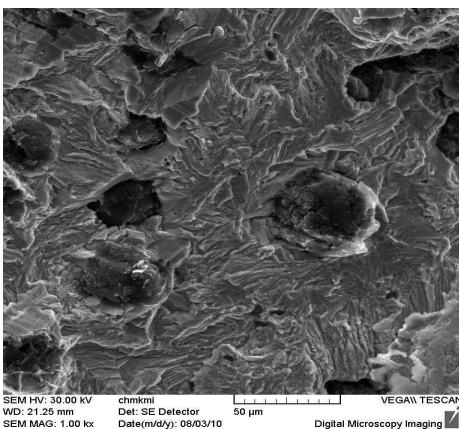
**Fig. 7** Fracture surface of fine ground specimens,  $S = 310$  MPa,  $N_f = 591\ 148$ , SEM



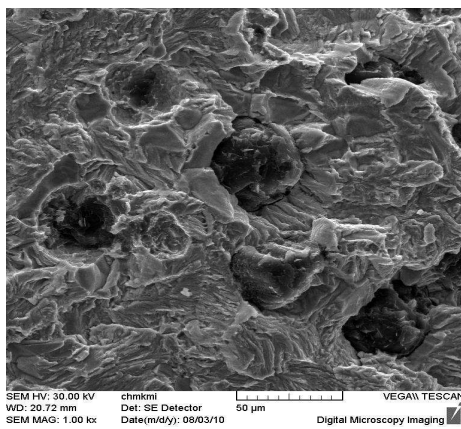
a) macroview of fracture surface



c) macroview of fracture surface



b) initiation region



d) initiation region

**Fig. 8** Fracture surface of rough ground specimens (a, b,  $S = 290$  MPa,  $N_f = 170\ 000$ ) and shot blast specimens (c, d,  $S = 250$  MPa,  $N_f = 381\ 042$ ), SEM

#### 4 Conclusions

The influence of surface conditions on the fatigue response of pearlite/ferrite nodular cast iron was investigated in this study. The following conclusions are reached:

- surface conditions have a strong effect on fatigue properties,
- a fine-ground surface generally provides the best fatigue behavior and the longest fatigue life,
- rough-grinding decreases the fatigue life compared to fine grinding,
- the as-cast surface shows the worst fatigue behavior,
- a shot-blasting treatment do not improve the fatigue strength.
- the transcrystalline continuous cleavage of pearlite is typical for all specimens,
- intercrystalline fracture of ferrite, locally transcrystalline ductile fracture of ferrite with sharp edges and transcrystalline continuous cleavage of pearlite with the rivers on the facets is also observed.

#### References

- [1] J. Davis: Cast irons/Metallurgy and Properties of Ductile Cast Irons, ASM Speciality Handbook, The Materials Information Society, USA ,1996.
- [2] R. Konečná, G. Nicoletto, B. Hadzimová, P. Lejček: Influence of temperature and micro-purity of ferrite on failure behavior of ductile iron, In: Fractography, Stará Lesná, 2003, p. 224-232.
- [3] R. Konečná, P. Lejček, G. Nicoletto, P. Bartuška: Materials Science and Technology, Vol. 22, 2006, No. 12, p. 1415-1421.
- [4] R. Konečná, G. Nicoletto, L. Collini, P. Bujnová: Acta Metallurgica Slovaca, Vol. 10, 2004, No. 1, p. 258-263.
- [5] P. Kapinová, R. Konečná, G. Nicoletto: Materials Engineering, Vol. 13, 2006, No. 4, p. 1-7.
- [6] J. Yamabe, M. Kobayashi: Fatigue & Fracture of Engineering Materials & Structures, Vol. 29, 2006, p. 403-415.
- [7] M. Endo: Journal of the Society of Materials Science (Japan), Vol. 38, p. 1139-1144.
- [8] S. Věchet, J. Kohout, O. Bokůvka: Fatigue properties of nodular cast iron, EDIS, Žilina, 2001, (in Czech).
- [9] R. I. Stephens, A. Fatemi, R. R. Stephens, H. O. Fuchs: Metal Fatigue in Engineering, 2<sup>nd</sup>. Edition, Wiley Interscience, New York, 2001.
- [10] Y. Murakami: Metal Fatigue: Effect of Small Defects and Nonmetallic Inclusions. Elsevier, UK, 2002.
- [11] R. Konečná, B. Záhorová, M. Matejka: Materials engineering, Vol. 7, 2000, No. 4, p. 27-34 (in Slovak).
- [12] G. Nicoletto, R. Konečná, L. Collini, P. Bujnová: Damage mechanisms in ferritic-pearlitic nodular cast iron, In.: Transactions of Famena, Zagreb, Vol. 28, 2004, ISSN 1333-1124.
- [13] P. Skočovský, A. Vaško: Quantitative evaluation of the nodular cast iron structure, EDIS, Žilina, 2007, (in Slovak).
- [14] O. Bokůvka, G. Nicoletto, L. Kunz, P. Palček, M. Chalupová: Low & High Frequency Fatigue Testing. CETRA, EDIS, Žilina, 2002.
- [15] F. Iacoviello, O. Di Bartolomeo, M. Cavallini: Resistance to propagation of fatigue cracks in austempered ductile irons, AIM National Conference, Vicenza, No. 19, 2004, (in Italy).
- [16] ASM handbook, vol. 12, Fractography. American Society of Materials International, USA, 1987.